Lattice evidence for the family of decoupling solutions of Landau gauge Yang-Mills theory

André Sternbeck[a,*], Michael Müller-Preussker[b]

[a] *Institut für Theoretische Physik, Universität Regensburg, 93040 Regensburg, Germany*
[b] *Institut für Physik, Humboldt-Universität zu Berlin, 12489 Berlin, Germany*

Abstract

We show that the low-momentum behavior of the Landau-gauge gluon and ghost propagators changes on the lattice if the gauge-fixing procedure favors Gribov copies with an exceptionally small lowest non-trivial eigenvalue of the Faddeev-Popov (FP) operator. Compared to random copies, the ghost propagator below 1 GeV grows stronger towards zero momentum on Gribov copies with a small lowest-lying FP eigenvalue, whereas the gluon propagator is more suppressed below 0.2 GeV. Above these momenta no dependence on Gribov copies is seen. Qualitatively, our data thus resembles the change of the gluon and ghost dressing functions, Z and J, with the boundary condition on $J(0)$, put forward by Fischer, Maas and Pawlowski [Annals Phys. 324 (2009) 2408].

Keywords: Landau gauge, gluon and ghost propagators, Gribov ambiguity, Faddeev-Popov eigenvalues

1. Introduction

Lattice calculations of the Landau-gauge gluon, ghost and quark propagators have attracted quite some interest during the last 15 years. Staunch supporters of pure lattice QCD (LQCD) may wonder about the enthusiasm with which such calculations have been performed and discussed in the past, in particular, as LQCD comes with the distinct advantage that one does not need to fix a gauge. This holds true, however, only as long as one is interested in gauge-invariant quantities. But besides LQCD there are also other (sometimes better suited) frameworks to tackle nonperturbative problems of QCD, and these require the exact knowledge of QCD's elementary two and three-point functions in Landau or other gauges.

Two continuum functional methods one has to mention here are the efforts to solve the infinite tower of Dyson-Schwinger equations (DSEs) of QCD or, likewise, the corresponding Functional Renormalization Group Equations (FRGEs) (see, e.g., the reviews [1–6] and references therein). Both these methods imply fixing a gauge (and often the Landau gauge is chosen for simplicity), but more importantly, these methods also require a truncation of the infinite system of equations to enable finding a numerical solution. These truncations are a potential source of error, which why corresponding (volume and continuum extrapolated) lattice results are so essential to render these truncations harmless or to even substitute parts of the DSE (or FRGE) solutions by (interpolated) nonperturbative data.

In what concerns the Landau-gauge gluon and ghost propagators, lattice results have helped much to improve truncations over the years. Currently, the continuum and lattice results overlap for a wide range of momenta, showing nice consistency among the so different approaches to QCD. Admittedly, the currently used truncations are still not perfect, as seen, for example, for the gluon propagator whose DSE solutions differ from the corresponding lattice or FRGE results in the intermediate momentum regime (i.e., for momenta 0.5 – 3 GeV), whereas FRGE and lattice results agree much better there (see, e.g., Fig. 2 in [7]). But this situation will certainly improve, as it did in the past.

Another regime that remains to be fully settled yet is the low (infrared) momentum regime. About the infrared behavior of the gluon and ghost propagators in Landau gauge there has been much dissent in the community and it is difficult to assess on the lattice also. Currently, all lattice studies agree upon a gluon propagator and ghost dressing function which are (most likely) finite in the zero-momentum limit (see, e.g., [8–16])[1]. DSE and FRGE studies [17–20], on the other hand, assert that this infrared behavior is not unique, but depends on an additional (boundary) condition on the ghost dressing function at zero momentum, $J(0)$. Explicitly, in Refs. [19, 20], it is shown that for $J^{-1}(0) = 0$ one finds the so-called *scaling* behavior for the gluon and ghost propagators at low momentum, as it was first found in [21], while for finite $J(0)$, one finds a family of *decoupling* solutions for the DSEs and FRGEs, in qualitative agreement with DSE solutions proposed in the studies of Refs. [22–27], and with lattice results. For momenta above 1 GeV both types of solutions are practically indistinguishable. We interpret this ambiguity in the infrared as a remnant of the Gribov ambiguity of the Landau gauge condition, which is lifted by fixing $J^{-1}(0)$ to a constant.

In this letter we will show that this one-parameter family of decoupling solutions can also be seen on the lattice, at least to the extent computational resources allow. After outlining some technical details in the next section and a discussion about the

*Corresponding author
Email address: andre.sternbeck@ur.de (André Sternbeck)

[1] Current lattice results for this regime are for finite lattice spacings and volumes only, and also the Gribov problem is only partially understood.

distribution of the lowest non-trivial eigenvalue of the Faddeev-Popov (FP) operator, λ_1, on different Gribov copies (Sect. 3), we will demonstrate in Sect. 4 that the decoupling-like behavior of the lattice gluon and ghost propagators can be changed by a (yet simple-minded) minimization of λ_1. Changes take place only in the low-momentum regime, but interestingly in a similar manner as shown in [19], where the condition on $J(0)$ was changed. Specifically, we show that on Gribov copies with very small λ_1 the ghost dressing function at low momenta is more enhanced than on random copies, while the gluon propagator is more suppressed.

We still find Gribov copies by a maximization of the lattice Landau-gauge functional, but we are not interested in finding Gribov copies with a large (local) gauge-functional value, but on copies with very small λ_1, irrespective of the functional value. Only then we see a stronger rising ghost dressing function and a more suppressed gluon propagator at low momentum. On Gribov copies with large gauge-functional values we see both being suppressed, consistent with what was found in the past [8, 28–31].

We should mention here that similar effects were seen for the B-gauges by Maas [32]. For these gauges, one selects Gribov copies based on the ratio of the ghost dressing function at a small and a large lattice momentum on a particular copy. By construction the ghost dressing function in these gauges is then clearly enhanced or suppressed at low momenta. It remains to be seen if corresponding effects become clear also for the gluon propagator.

2. Simulation details

Our study is based on 60 thermalized gauge field configurations, generated with the usual heatbath thermalization and Wilson's plaquette action for SU(2) lattice gauge theory. The lattice size is 56^4 and the coupling parameter $\beta = 2.3$. To reduce autocorrelations, configurations are separated by 2000 thermalization steps, each involving four over-relaxation and one heatbath step. For every configuration we generate at least $N_{\text{copy}} = 210$ gauge-fixed (Gribov) copies, all fixed to lattice Landau gauge using an optimally-tuned over-relaxation algorithm for the gauge fixing. To ensure these Gribov copies are all distinct, the gauge-fixing algorithm always starts from a random gauge transformation field. Interestingly, for all these 60×210 gauge-fixing attempts we only found one Gribov copy twice.

With the help of PARPACK [33] we then calculate the lowest three (non-trivial) eigenvalues $0 < \lambda_1 < \lambda_2 < \lambda_3$ of the Faddeev-Popov (FP) operator of every Gribov copy, and classify them by their value for λ_1. The Gribov copy with lowest λ_1 (considered for each configuration separately) is labeled *lowest copy* (ℓc). The first generated copy, irrespective of λ_1, gets the label *first copy* (fc). It represents an arbitrary (random) Gribov copy of a configuration. To compare with former lattice studies on the problem of Gribov copies we also reintroduce the label *best copy* (bc). It refers to that copy with the best (largest) gauge functional value

$$F_U[g] = \frac{1}{4V} \sum_x \sum_{\mu=1}^{4} \mathfrak{Re}\, \mathrm{Tr}\, g_x U_{x\mu} g^\dagger_{x+\hat{\mu}} \,. \tag{1}$$

for a particular gauge configuration $U \equiv \{U_{x\hat{\mu}}\}$. Here $g \equiv \{g_x\}$ denotes one of the many gauge transformation fields fixing U to Landau gauge.

On those three sets of Gribov copies we calculate the SU(2) gluon and ghost propagators following standard recipes. That is, the gluon propagator is calculated for every lattice momentum using a fast Fourier transformation and the ghost propagator by using the plane-wave method for selected momenta. To accelerate the latter we use the preconditioned conjugate gradient algorithm of [8]. As a by-product of this calculation we also obtain the renormalization constant, $\widetilde{Z}_1$, of the ghost-ghost-gluon (gh-gl) vertex in Landau gauge for zero incoming gluon momentum. For more details on lattice Landau gauge and the calculation of the propagators and $\widetilde{Z}_1$ the reader may refer to Refs. [8, 34–36] and references therein.

When quoting momenta in physical units we adopt the usual definition $ap_\mu(k_\mu) = 2\sin\left(\pi k_\mu / L_\mu\right)$ [with $k_\mu \in (-L_\mu/2, L_\mu/2]$ and $L_\mu \equiv 56$], assume for the string tension $\sqrt{\sigma} = 440\,\text{MeV}$ and use $\sigma a^2 = 0.145$ for $\beta = 2.3$ from Ref. [37], where a denotes the lattice spacing.

3. Distribution of λ_1

Before comparing the propagator data for the different types of Gribov copies, it is instructive to look at the distribution of λ_1 on all copies first. In Fig. 1 we show this eigenvalue distribution (in lattice units) for $N_{\text{cp}} = 210$ Gribov copies. There, the big panel shows it separately for each of the 60 gauge configurations and the small panel (on top) for all configurations together as a histogram. One sees that for most of the copies λ_1 takes values between 0.5×10^{-3} and 1.9×10^{-3}, mostly between 1.5×10^{-3} and 1.7×10^{-3}, but for some configurations there are also copies with an exceptionally small value for λ_1, a value ($\lambda_1 < 10^{-4}$) far below the values found for the other copies. With our simple (brute-force) approach we are rather limited in finding more of these exceptional copies. The gauge-fixing and calculation of eigenvalues on a 56^4 lattice is computational quite demanding, and a more sophisticated gauge-fixing algorithm—one which would automatically select that Gribov copy with the smallest (or at least with small) λ_1—does not exist. But it would be interesting to know if for each configuration a Gribov copy with such an exceptionally small λ_1 exists.

For a few configurations we generated more than 210 Gribov copies. These allow us now to have a closer look at the distribution of λ_1 and to demonstrate that this number of copies is sufficient to resemble the distribution's shape for our lattice parameters ($\beta = 2.3$, 56^4).

Typical snapshots of this distribution for different N_{cp} are shown in Fig. 2, from left to right for three arbitrarily selected configurations. There, the middle panels illustrate how the range of λ_1-values gets populated when increasing N_{cp}; shown

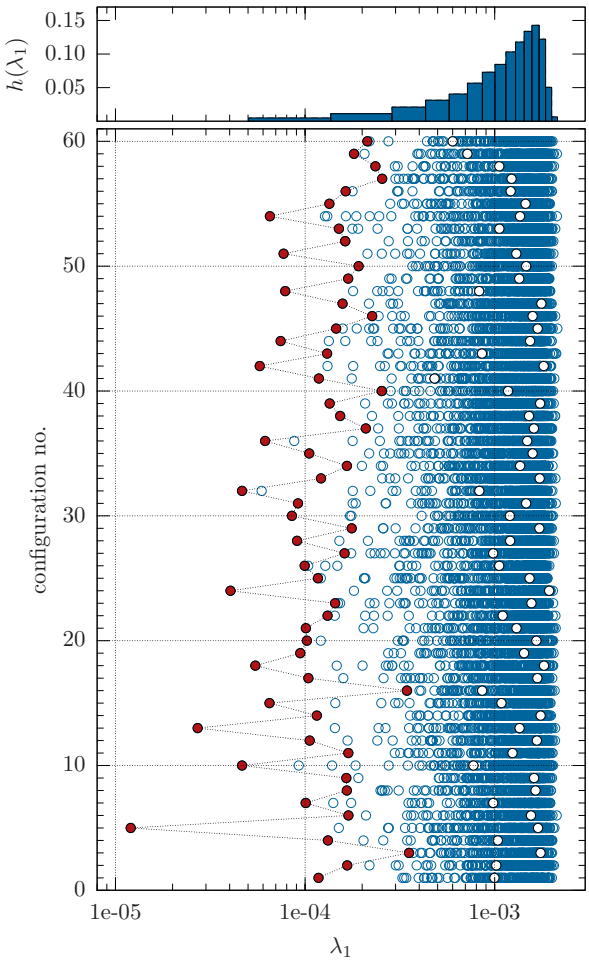

Figure 1: Distribution of λ_1 (in lattice units) for 210 Gribov copies, shown separately for 60 thermalized gauge configurations (ordinate). Full red (white) circles mark the eigenvalue on ℓc (fc) copies. The small top panel shows as a histogram for λ_1 including all values found.

are distributions for $N_{\rm cp} = 70$, 210, 420 and 500 Gribov copies. The top panels show the corresponding histograms, filled with the respective symbol color used in the middle panels. To ease the comparison, these histograms are all normalized with respect to $N_{\rm cp} = 420$.

From these histograms we see that the individual (configuration-wise) distributions of λ_1 are asymmetric and negatively skewed, similar to what we have just seen for the overall distribution in Fig. 1. Moreover, we see that at least 200 Gribov copies are needed to reach at an approximate shape for the distribution. This number of copies seems to be also sufficient (for the given lattice parameters) to find a copy with a very small λ_1, even though it is unlikely that this copy is the one with the smallest λ_1 overall.

We are thus in a good position to analyze the relation of a very-low λ_1 and the low-momentum behavior of the gluon and ghost propagator.

The attentive reader may have noticed the bottom panels of Fig. 2. These show correlation plots of λ_1 versus the gauge functional $F_U[g]$, always for the largest available number of Gribov copies ($N_{\rm cp} = 420$ or 500) for the respective configuration. In former lattice studies on the infrared behavior of the gluon and ghost propagators (e.g., [12, 13, 30, 38]), gauge-fixing algorithms were often designed to find copies with comparably large $F_U[g]$, in the hope these copies are closer to the fundamental modular region than a set of random copies can be. Gribov copies which globally maximize the gauge functional are elements of the fundamental modular region, and in the continuum the common boundary of this region and the Gribov horizon (the set of Gribov copies with $\lambda_1 = 0$) is expected to dominate the path integral in the thermodynamic limit [39–41]. One might thus expect that a small value for λ_1 is correlated to a large value for $F_U[g]$. Looking at the distributions for λ_1 and $F_U[g]$ (Fig. 2), we find, however, there is no obvious correlation between them. There are copies with small λ_1 and small $F_U[g]$, but at the same time there are also copies with small λ_1 and large $F_U[g]$, and vice versa.

4. λ_1 and the gluon and ghost propagator

Next we look at the correlation of λ_1 and the gluon and ghost propagator at low momenta. For the gluon propagator $D(k)$ [or its dressing function $Z(k) = p^2 D(k)$] there is actually no direct relationship between its momentum dependence and the spectrum of the FP operator, besides that it is gauge-dependent and so may change if the lattice Landau gauge condition is supplemented by a condition on λ_1.

The ghost propagator $G(k)$ [or its dressing function $J(k) = p^2 G(k)$], on the other hand, should be affected stronger. Given its spectral decomposition in SU(2),

$$G(k) = \frac{1}{3} \sum_{i=1}^{3V-3} \frac{\vec{\Phi}_i(k) \cdot \vec{\Phi}_i(-k)}{\lambda_i} \,, \qquad (2)$$

it is plausible that Gribov copies with very small λ_1 yield larger values for G than copies where λ_1 is comparably large, possibly even configuration-wise. Though this is not as simple as it seems at first sight, because λ_1 and the corresponding eigenfunction $\Phi_1(k)$ contribute only a minor fraction to $G(k)$ and this fraction even shrinks the larger the lattice momentum $a^2 p^2(k)$ (see Ref. [42], in particular Fig. 6 therein). From [43] (Fig. 1) we learn that this fraction seems to increase with volume.

For a few gauge configurations we have data for the gluon and ghost propagator for all Gribov copies. It allows us to check if there is a direct correlation between λ_1 and the gluon and ghost propagator at low momenta, comparing different Gribov copies of the same configuration. Looking at this data reveals, however, no immediate correlation: A Gribov copy with a smaller λ_1 not necessarily yields a larger ghost propagator than a copy with a somewhat larger λ_1. Similar we find for the gluon propagator.

Nonetheless, when looking at these correlations more broadly, that is on average for the whole gauge ensemble, we see a clear trend: Gribov copies with very small λ_1 tend to yield a larger ghost propagator at low momentum, than copies with

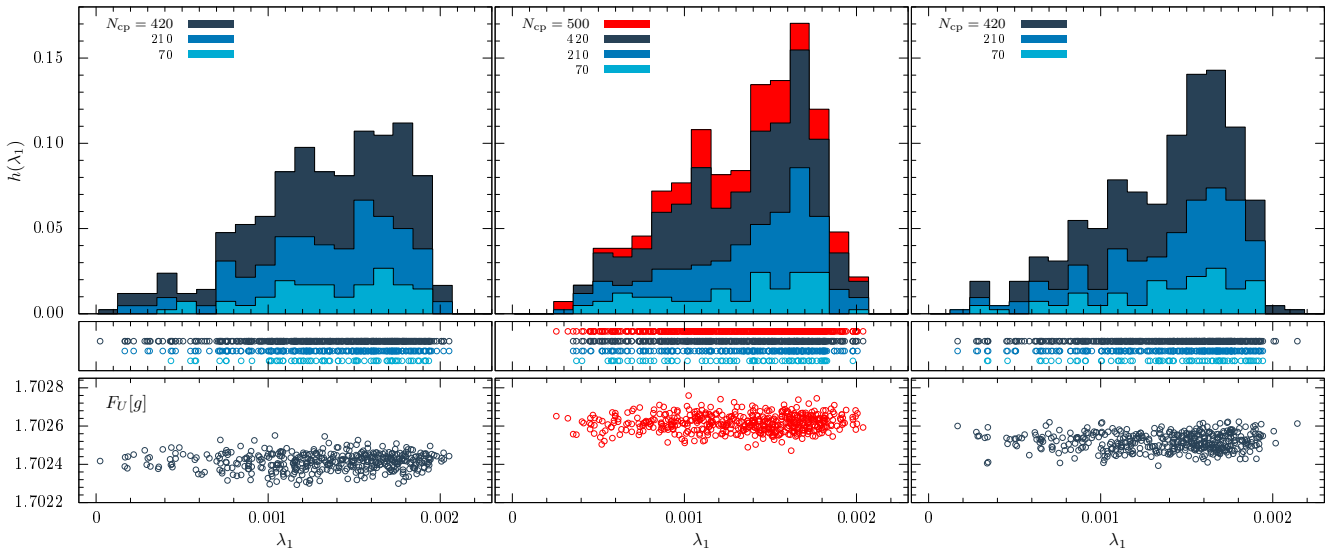

Figure 2: Top panels: histogram of the eigenvalue distribution of λ_1 for different numbers N_{cp} of Gribov copies. From left to right, each panel is for one gauge configuration. All histograms are normalized such that the sum of bars is one for $N_{cp} = 420$ copies. The middle panels show the corresponding scattering of λ_1 for the different N_{cp}, and the lower panels show scatter plots of λ_1 versus the gauge functional values $F_U[g]$ for the respective largest N_{cp}.

large λ_1. This anti-correlation is smaller the larger the momentum, and is also considerably smaller for the gluon propagator at same momentum.

We clearly see both these correlations when comparing averaged lattice data as shown in Fig. 3. There the left panels compare the momentum dependence of the SU(2) ghost dressing function (top) and the gluon propagator (bottom) as obtained on first, lowest and best copies of our gauge ensemble (refer to Sect. 2 for this classification). The right panels confront the corresponding data for the strong coupling constant,

$$\alpha^{\mathsf{MM}}_{\mathrm{SU(2)}} = \frac{g_0^2}{4\pi}\, Z \cdot J^{\,2}\,, \tag{3}$$

here in the Minimal MOM scheme for SU(2) Landau gauge [44], and of the inverse renormalization constant $\widetilde{Z}_1^{-1}$ of the gh-gl vertex with zero incoming gluon momentum.

Looking first at the first-copy (*fc*) data points (black open circles in Fig. 3), we see these behave as expected [10, 11, 13, 30, 31]: The ghost dressing function and the gluon propagator increase with decreasing momentum and tend to reach a plateau at very low momentum, while $\alpha^{\mathsf{MM}}_{\mathrm{SU(2)}}$ grows with decreasing momentum down to about $a^2p^2 = 0.2$ ($p \approx 0.5\,\mathrm{GeV}$) below which it falls off again with momentum. Also $\widetilde{Z}_1^{-1}$ is found as expected: $\widetilde{Z}_1^{-1} \to 1$ for large momenta, as it should, and for intermediate momenta we see its characteristic hump [34, 35, 45].

But the most interesting data in Fig. 3 is the lowest-copy (ℓc) data (red full squares). The ℓc data points, for example, for the ghost dressing function clearly deviate upwards from the respective *fc* data below $a^2p^2 = 0.5$, while for the gluon propagator these systematically deviate downwards below $a^2p^2 = 0.03$. These deviations then yield a coupling, $\alpha^{\mathsf{MM}}_{\mathrm{SU(2)}}$, whose running is slightly upwards shifted below $a^2p^2 = 0.5$. Admittedly, compared to the ghost dressing function, the effect for the gluon propagator is small, but we find that it becomes more and more pronounced when increasing statistics. Looking, for instance, at half the number of configurations the effect is less significant than for the full set. So we think the effects we find for both propagators and $\alpha^{\mathsf{MM}}_{\mathrm{SU(2)}}$ are not statistical artifacts, but result from our selection of Gribov copies with very small λ_1.

For completeness, we also show the corresponding best-copy (*bc*) data in Fig. 3 (blue crosses). Comparing this with the *fc* data, we find the expected suppression of the *bc* data for the ghost and gluon propagator at low momentum which is then also seen for $\alpha^{\mathsf{MM}}_{\mathrm{SU(2)}}$. Similar was seen for the *bc* data in [12, 30], although there the effect was even bigger when using the FSA gauge-fixing, a special combination of the simulated annealing and over-relaxation algorithm for gauge-fixing and $Z(2)$ flips.

For all three types of Gribov copies, we find that $\widetilde{Z}_1^{-1}$ remains almost unaffected (see lower right panel of Fig. 3). There are small upward shifts for the ℓc data at small and at large momentum (there also for the *bc* data), but these shifts are all within (statistical) errors, besides at lowest momentum. This certainly deserves further study, because at large momenta $\widetilde{Z}_1 \to 1$ for all types of copies [44, 46], while at small momenta $\widetilde{Z}_1$ is expected to approach one or at least a value close to one [17].

5. Summary and conclusion

We have demonstrated that the low-momentum behavior of the Landau-gauge gluon and ghost propagators can be changed on the lattice by an additional constraint on the lowest-lying (non-trivial) eigenvalue, λ_1, of the FP operator. If the lattice Landau gauge fixing is tuned to find Gribov copies with a very small λ_1, the ghost dressing function gets more enhanced towards the infrared momentum limit and the gluon propagator more suppressed. The combined effect then yields a coupling constant $\alpha^{\mathsf{MM}}_{\mathrm{SU(2)}}$ whose running is slightly upwards shifted for

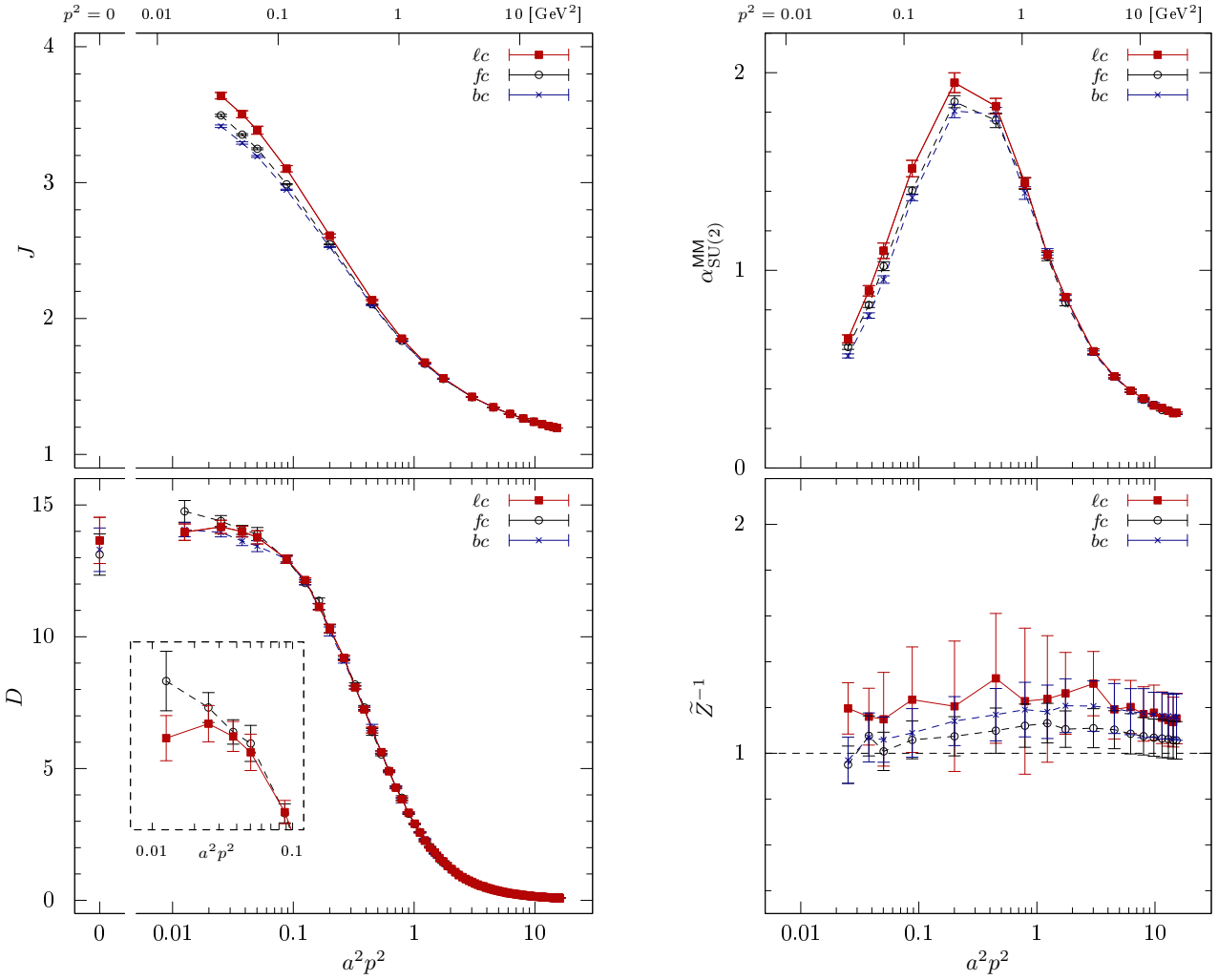

Figure 3: Ghost dressing function (top left), gluon propagator (bottom left), the coupling $\alpha^{\mathsf{MM}}_{\mathrm{SU}(2)}$ (top right) and the inverse renormalization constant of the gh-gl-vertex (bottom right); all versus lattice momentum squared, in lattice units and for SU(2), and no renormalization has been applied. Open circles (filled squares, crosses) refer to data on fc (ℓc, bc) copies. The lower left panel also shows a zoomed-in plot to improve visibility of the low-momentum region. Note the different scales for the x-axis (log and linear) in the left panels and the corresponding physical momenta above the top panels.

momenta below 0.7 GeV. In contrast, Gribov copies with a large gauge functional value tend to suppress instead both propagators and $\alpha^{\mathsf{MM}}_{\mathrm{SU}(2)}$ at low momentum.

These Gribov-copy effects are not noticeable at momenta above 1 GeV. Also, these effects cause only a quantitative but no qualitative change of both these propagators at low momentum. Their modified momentum dependences are still of decoupling type. But interestingly, the change we find with λ_1 looks very much alike the change of the gluon and ghost dressing functions, Z and J, with the (boundary) condition on $J(0)$ as found in [19][2]. Looking at Fig. 5 therein, one sees that if $J(0)$ is fixed to a larger value the ghost dressing function below 1 GeV is enhanced, while the gluon dressing function below 0.2 GeV is decreased. One further sees that the effect is stronger for the ghost than for the gluon dressing function (compared at same momentum), and that the deviation of the strong coupling constant appears below and slightly above the position of its maximum at a momentum of about 0.5 GeV.

This is exactly what we find from our ℓc data, suggesting that the constraint on $J(0)$, used in [19] to lift the Gribov ambiguity of Landau gauge, can be mimicked on the lattice by supplementing the lattice Landau-gauge condition by a constraint on λ_1.

Strictly speaking, our results are for SU(2) only, but similar should be expected for SU(3). The propagators for these gauge groups differ only little [11, 47]. SU(2) and the rather coarse 56^4 lattice ($\beta = 2.3$) was chosen here on purpose, because it has allowed us to get (with reasonable computer time) data for the gluon propagator and the ghost dressing function where their momentum dependence starts to become flat, and this for a sufficient number of Gribov copies (at least 200 per config.) such that a correlation between λ_1 and both propagators can be seen.

[2]Note that in [19] the ghost dressing function is denoted G.

For a future study, we suggest to cross-check our results at lower momenta, in particular, for the gluon propagator whose low-momentum behavior changes only little, if one constrains λ_1, or $J(0)$ in the continuum. Also 3-point functions of gluon and ghost fields should be checked, and what changes when adding fermions. Note that larger lattice sizes and smaller lattice spacings will perhaps also affect the low-momentum behavior on any finite lattice [16, 36]. Such calculations will thus become expensive very quickly—especially, if Gribov copies with exceptionally small λ_1 still have to be found by chance. Algorithmic improvements would therefore be quite helpful. For example, a gauge-fixing algorithm that automatically selects Gribov copies with very small λ_1.

Let us comment on the "rigorous bounds" introduced in [43, 48] to control the infinite-volume extrapolations of lattice data for the gluon and ghost propagator. Since these bounds are composed of the lattice gluon field (for the gluon propagator), and of λ_1 and the eigenmode $\vec{\Phi}_1$ (for the ghost propagator), these will suffer similar Gribov problems as seen for the propagators here. For a particular lattice implementation of Landau-gauge Yang-Mills theory and a particular selection of Gribov copies these bounds will certainly constrain the lattice data, but one should keep in mind these bounds may change when using others.

With the current lattice implementation of Landau-gauge Yang-Mills theory, one seems to be able to realize different decoupling-type solutions for the propagators by supplementing the lattice Landau-gauge condition by an additional constraint, as, e.g., the one here or in [32], but it will perhaps be impossible to find the scaling solution on a finite lattice. Even if we were able to find for every gauge configuration that Gribov copy with the smallest λ_1, this eigenvalue and all the others would still be non-zero, i.e., this copy is not on the Gribov horizon. It remains to be seen if for such an approach the scaling behavior can then appear in the limit of infinite volume and zero lattice spacing.

Acknowledgments

This work was supported by the European Union under the Grant Agreement number IRG 256594. We thank A. Maas and J. Pawlowski for helpful comments and discussions, and the HLRN (Germany) for the generous support of computing time.

References

[1] R. Alkofer, L. von Smekal, Phys.Rept. 353 (2001) 281. arXiv:hep-ph/0007355.
[2] J. M. Pawlowski, Annals Phys. 322 (2007) 2831–2915. arXiv:hep-th/0512261.
[3] H. Gies arXiv:hep-ph/0611146.
[4] C. S. Fischer, J.Phys. G32 (2006) R253–R291. arXiv:hep-ph/0605173.
[5] C. Roberts, M. Bhagwat, A. Holl, S. Wright, Eur.Phys.J.ST 140 (2007) 53–116. arXiv:0802.0217.
[6] C. D. Roberts arXiv:1203.5341.
[7] C. S. Fischer, A. Maas, J. M. Pawlowski, PoS CONFINEMENT8 (2008) 043. arXiv:0812.2745.
[8] A. Sternbeck, E.-M. Ilgenfritz, M. Müller-Preussker, A. Schiller, Phys.Rev. D72 (2005) 014507. arXiv:hep-lat/0506007.
[9] P. Boucaud, J. Leroy, A. Le Yaouanc, A. Lokhov, J. Micheli, et al. arXiv:hep-ph/0507104.
[10] A. Cucchieri, T. Mendes, PoS LAT2007 (2007) 297. arXiv:0710.0412.
[11] A. Sternbeck, L. von Smekal, D. Leinweber, A. Williams, PoS LAT2007 (2007) 340. arXiv:0710.1982.
[12] V. Bornyakov, V. Mitrjushkin, M. Müller-Preussker, Phys.Rev. D79 (2009) 074504. arXiv:0812.2761.
[13] I. Bogolubsky, E.-M. Ilgenfritz, M. Müller-Preussker, A. Sternbeck, Phys.Lett. B676 (2009) 69–73. arXiv:0901.0736.
[14] O. Oliveira, P. Silva, Phys.Rev. D79 (2009) 031501. arXiv:0809.0258.
[15] J. M. Pawlowski, D. Spielmann, I.-O. Stamatescu, Nucl.Phys. B830 (2010) 291–314. arXiv:0911.4921.
[16] O. Oliveira, P. J. Silva arXiv:1207.3029.
[17] C. Lerche, L. von Smekal, Phys.Rev. D65 (2002) 125006. arXiv:hep-ph/0202194.
[18] D. Zwanziger, Phys.Rev. D65 (2002) 094039. arXiv:hep-th/0109224.
[19] C. S. Fischer, A. Maas, J. M. Pawlowski, Annals Phys. 324 (2009) 2408–2437. arXiv:0810.1987.
[20] F. J. Llanes-Estrada, R. Williams, Phys.Rev. D86 (2012) 065034. arXiv:1207.5950.
[21] L. von Smekal, R. Alkofer, A. Hauck, Phys.Rev.Lett. 79 (1997) 3591–3594. arXiv:hep-ph/9705242.
[22] A. Aguilar, A. Natale, JHEP 0408 (2004) 057. arXiv:hep-ph/0408254.
[23] P. Boucaud, T. Bruntjen, J. Leroy, A. Le Yaouanc, A. Lokhov, et al., JHEP 0606 (2006) 001. arXiv:hep-ph/0604056.
[24] D. Dudal, S. Sorella, N. Vandersickel, H. Verschelde, Phys.Rev. D77 (2008) 071501. arXiv:0711.4496.
[25] A. Aguilar, D. Binosi, J. Papavassiliou, Phys.Rev. D78 (2008) 025010. arXiv:0802.1870.
[26] P. Boucaud, J.-P. Leroy, A. L. Yaouanc, J. Micheli, O. Pene, et al., JHEP 0806 (2008) 012. arXiv:0801.2721.
[27] P. Boucaud, J. Leroy, A. Le Yaouanc, J. Micheli, O. Pene, et al., JHEP 0806 (2008) 099. arXiv:0803.2161.
[28] T. Bakeev, E.-M. Ilgenfritz, V. Mitrjushkin, M. Müller-Preussker, Phys.Rev. D69 (2004) 074507. arXiv:hep-lat/0311041.
[29] I. Bogolubsky, V. Bornyakov, G. Burgio, E. Ilgenfritz, M. Müller-Preussker, et al., Phys.Rev. D77 (2008) 014504. arXiv:0707.3611.
[30] V. Bornyakov, V. Mitrjushkin, M. Müller-Preussker, Phys.Rev. D81 (2010) 054503. arXiv:0912.4475.
[31] I. Bogolubsky, E.-M. Ilgenfritz, M. Müller-Preussker, A. Sternbeck, PoS LAT2009 (2009) 237. arXiv:0912.2249.
[32] A. Maas, Phys.Lett. B689 (2010) 107–111. arXiv:0907.5185.
[33] R. Lehoucq, K. Maschhoff, D. Sorensen, C. Yang, Arpack software. URL http://www.caam.rice.edu/software/ARPACK/
[34] A. Cucchieri, T. Mendes, A. Mihara, JHEP 0412 (2004) 012. arXiv:hep-lat/0408034.
[35] A. Sternbeck, The Infrared behavior of lattice QCD Green's functions, Ph.D. thesis, Humboldt-University Berlin (2006). arXiv:hep-lat/0609016.
[36] A. Sternbeck, L. von Smekal, Eur.Phys.J. C68 (2010) 487–503. arXiv:0811.4300.
[37] K. Langfeld, Phys.Rev. D76 (2007) 094502. arXiv:0704.2635.
[38] I. Bogolubsky, G. Burgio, M. Müller-Preussker, V. Mitrjushkin, Phys.Rev. D74 (2006) 034503. arXiv:hep-lat/0511056.
[39] D. Zwanziger, Nucl.Phys. B412 (1994) 657–730.
[40] D. Zwanziger, Nucl.Phys. B518 (1998) 237–272.
[41] D. Zwanziger, Phys.Rev. D69 (2004) 016002. arXiv:hep-ph/0303028.
[42] A. Sternbeck, E.-M. Ilgenfritz, M. Müller-Preussker, Phys.Rev. D73 (2006) 014502. arXiv:hep-lat/0510109.
[43] A. Cucchieri, T. Mendes, Phys.Rev. D78 (2008) 094503. arXiv:0804.2371.
[44] L. von Smekal, K. Maltman, A. Sternbeck, Phys.Lett. B681 (2009) 336–342. arXiv:0903.1696.
[45] A. Cucchieri, A. Maas, T. Mendes, Phys.Rev. D77 (2008) 094510. arXiv:0803.1798.
[46] J. Taylor, Nucl.Phys. B33 (1971) 436–444.
[47] A. Cucchieri, T. Mendes, O. Oliveira, P. Silva, Phys.Rev. D76 (2007) 114507. arXiv:0705.3367.
[48] A. Cucchieri, T. Mendes, Phys.Rev.Lett. 100 (2008) 241601. arXiv:0712.3517.